J. Chem. Sci. Vol. 128, No. 4, April 2016, pp. 573–588. © Indian Academy of Sciences.
DOI 10.1007/s12039-016-1046-8

Kinetics of the thermal decomposition of tetramethylsilane behind the reflected shock waves between 1058 and 1194 K

A PARANDAMAN and B RAJAKUMAR*
Department of Chemistry, Indian Institute of Technology Madras, Chennai 600 036, India
e-mail: rajakumar@iitm.ac.in

MS received 16 September 2015; revised 31 December 2015; accepted 4 January 2016

Abstract. Thermal decomposition of tetramethylsilane (TMS) diluted in argon was studied behind the reflected shock waves in a single pulse shock tube (SPST) in the temperature range of 1058–1194 K. The major products formed in the decomposition are methane (CH_4) and ethylene (C_2H_4); whereas ethane and propylene were detected in lower concentrations. The decomposition of TMS seems to be initiated via Si-C bond scission by forming methyl radicals (CH_3) and trimethylsilyl radicals ($(CH_3)_3Si$). The total rate coefficients obtained for the decomposition of TMS were fit to Arrhenius equation in two different temperature regions 1058–1130 K and 1130–1194 K. The temperature dependent rate coefficients obtained are k_{total} (1058–1130 K) $= (4.61 \pm 0.70) \times 10^{18} \exp(-(79.9\,\text{kcal mol}^{-1} \pm 3.5)/RT)\ \text{s}^{-1}$, k_{total} (1130-1194 K) $= (1.33 \pm 0.19) \times 10^{6} \exp(-(15.3\,\text{kcal mol}^{-1} \pm 3.5)/RT)\ \text{s}^{-1}$. The rate coefficient for the formation of CH_4 is obtained to be $k_{methane}$ (1058–1194 K) $= (4.36 \pm 1.23) \times 10^{14} \exp(-(61.9\,\text{kcal mol}^{-1} \pm 4.9)/RT)\ \text{s}^{-1}$. A kinetic scheme containing 21 species and 38 elementary reactions was proposed and simulations were carried out to explain the formation of all the products in the decomposition of tetramethylsilane.

Keywords. tetramethylsilane; single pulse shock tube; decomposition; shock wave; simulation.

1. Introduction

Tetramethylsilane (TMS) is the simplest carbosilane, broadly used in semiconductor industry as a precursor for preparation of silicon carbide (SiC) through chemical vapor deposition (CVD) technique.[1,2] Silicon carbide (SiC) is used in various applications because of its important properties such as high heat resistance, high thermal conductivity and to withstand high voltage.[3] It is a well-known promising substrate material for power electronic devices and light emitting devices (LED).[4] Good quality SiC films can be grown on Si substrates by pyrolyzing single organosilane precursors, which contain bonds between Si and C atoms, such as methylsilane (CH_3SiH_3), tetramethylsilane ($(CH_3)_4Si$), methyltrichlorosilane (CH_3SiCl_3).[5–7] Among them, TMS has more advantages as a precursor. It is considered as a safe, non-explosive and non-corrosive precursor material that can be easily handled in the experiments.[8]

As TMS is the source to provide Si, our initial focus would be on the resultant products from TMS formed via Si-C bond breaking reactions. Seo *et al.*,[9] produced 3C-SiC(111) films on Si substrates from TMS, employing a rapid thermal CVD technique above 1000°C. They reported that TMS decomposed into H and Si atoms and hydrocarbon gases such as CH_4, C_2H_2, and C_2H_4 at high temperatures. Herlin *et al.*,[10] studied the growth mechanism of SiC on a graphite susceptor in a low-pressure cold wall reactor. They found that dissociation of TMS releases H atoms, various Si-containing species and hydrocarbons. In all these experiments no consistent conclusions about the products from TMS decomposition were made. The detailed analysis on products and clear understanding of mechanism is the main focus of the present study. Various precursors such as TMS, diethylsilane and tripropylsilane are commonly used in the preparation of SiCvia CVD. Previous investigations by Avigal and Schieber[11] reported that, SiC was obtained from TMS either in an inert (He) atmosphere or reducing (H_2) atmosphere in the temperatures between 700 and 1400°C. Several experimental studies reported that TMS was used for conventional CVD experiments[12,13] to produce solid materials of high efficiency and high purity. In the process of CVD at high temperature with TMS, the subject of gas phase contribution to the overall process cannot be neglected.

The spontaneous flammability of certain alkylsilanes suggest that metal - carbon bonds are more susceptible to oxidation than carbon - hydrogen or carbon - carbon bonds. Schalla *et al.*,[14] studied the temperature required for the rapid oxidation or explosion of alkylsilanes (including TMS) air mixtures at one atmospheric

*For correspondence

pressure and they have reported the explosion limits of a series of alkylsilanes. SiC was also synthesized by injecting mixture of carrier gas (H_2, He, N_2 and C_2H_4) and TMS into hot burned gas downstream of a fuel rich hydrocarbon oxygen flame.[15] Cullis *et al.*,[16] studied the possibility of silicon containing compounds including TMS as anti-knock additives in engines and they have concluded that none of these silicon compounds are viable anti-knock additives in fuels.

TMS has simple carbosilane structure and is used as a model monomer for studying the reactivity of silylmethyl groups in plasma polymerization reactions.[17] The thermal decomposition studies on TMS were conducted by Helm and Mack[18] in a static reactor and they have reported that the reaction was unimolecular and homogeneous at pressures above 100 Torr in the temperature range of 932–993 K. The thermal decomposition studies on TMS were also carried out by Clifford *et al.*,[19] in a linear flow system in the temperature range of 810–980 K, using gas chromatography for the detection of reactant and products. They have reported the first order rate coefficient for the formation of methane to be $k = 2.0 \times 10^{14} \exp(-67.9\,\text{kcal mol}^{-1}/\text{RT})\text{s}^{-1}$. The decomposition of TMS was also studied by Baldwin *et al.*,[20] in a pulsed stirred-flow system between 800 and 1055 K using GLC-Mass spectrometry as a detection system. They have reported two sets of rate coefficients for the formation of CH_4 from the decomposition of TMS. The first order rate coefficient for the formation of CH_4 in the temperature range of 840-950K was reported to be $k = 1.58 \times 10^{11} \exp(-57.4\,\text{kcal mol}^{-1}/\text{RT})\ \text{s}^{-1}$, and for temperature range of 955–1055 K, the rate coefficient reported was $k = 3.98 \times 10^{17} \exp(-85.2\,\text{kcal mol}^{-1}/\text{RT})\ \text{s}^{-1}$, where the activation energies are given in kcal mol^{-1}. Taylor *et al.*,[21] studied the pyrolysis of tetramethyl derivatives of silicon, germanium and tin using a wall less reactor under both homogeneous and heterogeneous (surface) conditions. They have reported the rate coefficient for the pyrolysis of TMS in homogeneous conditions to be $k = 1.29 \times 10^{14} \exp(-72.0\,\text{kcal mol}^{-1}/\text{RT})\ \text{s}^{-1}$ and in surface conditions it was reported to be $k = 3.16 \times 10^{12} \exp(-61.0\,\text{kcal mol}^{-1}/\text{RT})\ \text{s}^{-1}$. Although the decomposition of TMS were studied earlier in a wide temperature range of 800–1055 K by various groups, complete mechanistic studies were not reported so far, to the best of our knowledge.

In the present investigation, we report the complete thermal decomposition of TMS in the temperature range of 1058–1194 K. A most plausible mechanism for the decomposition is proposed and simulated. The decomposition pathways and the mechanistic approach are discussed in this paper. In the present study, the solid products and their growth were not monitored. However, formation of lower hydrocarbon products and their gas phase contribution to the overall reaction were focused. Silicon containing products were not observed from post shock mixture analysis. If TMS was extensively used as a precursor for preparation of SiC, lower hydrocarbons along with solid SiC will be formed at higher temperatures. Si-C bond breaking is the most important channel and the primary step in the pyrolysis of TMS because Si-C bond energy[20] is 85 kcal mol^{-1} which is lower than C-H bond dissociation[22] energy (99.2 kcal mol^{-1}).

2. Experimental

The thermal decomposition of TMS was studied behind the reflected shock waves in a single pulse shock tube (SPST).A schematic diagram of the SPST used in this study is given in figure 1. A 50.8 mm i.d. SPST consisting of a 3440 mm long driven section and 1290 mm length driver section was used in the present investigation. The driver section was separated from the driven section by an aluminum diaphragm.

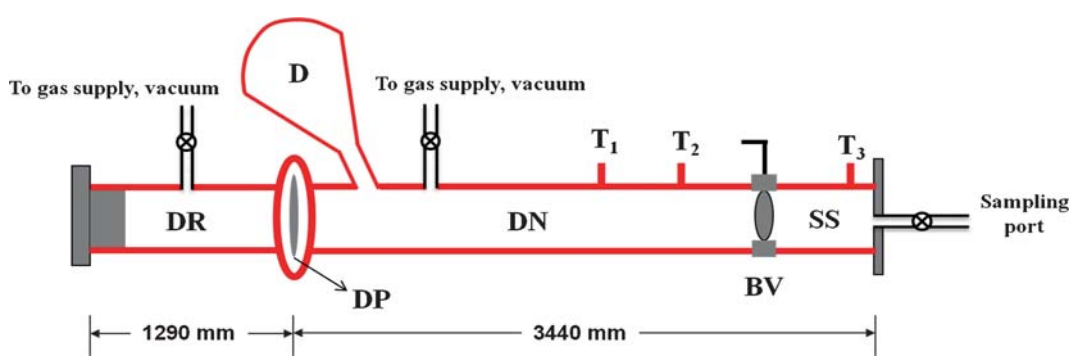

Figure 1. Schematic diagram of the single pulse shock tube used in the present study. DR-driver section, DN-driven section, SS-sample section, BV-ball valve, DP-diaphragm, T_1, T_2 and T_3-pressure transducers, D- dump tank.

A confined reaction zone was created towards the end of the shock tube by incorporating a ball valve. This is to ensure that all the test molecules are exposed to the reflected shock wave. The success of shock tube technique depends on exposing a reaction mixture to a single high temperature pulse, in which the reactants are allowed to remain at reaction conditions (constant temperature) for a closely controlled period of time, i.e., reaction time, followed by rapid cooling through the action of strong rarefaction wave. The cooling rate must be sufficiently high to effectively freeze the reaction. The problem of a variable dwell time may be substantially reduced by introducing a small test section in the shock tube. The lengths of the driver and driven sections were chosen in such a way that the expansion fan cools the heated sample before the reflected wave meets the contact surface. The location of the ball valve (550 mm from the end of the driven section) was chosen to ensure that the compressed test gas occupies a region around the pressure transducer. Hence, the dwell time measured from the pressure trace is very close to the reaction time, i.e., the time for which the molecules were kept at the temperature behind the reflected wave, T_5. The smaller test section created using a ball valve will facilitate fixing the dwell time.[23–25] In fact, the progress of the shock wave will be influenced if, there is a sudden and significantly larger change in the specific heat ratios across the ball valve. The concentration of the sample is chosen in such a way that the specific heat ratio remains almost constant after dilution with the same buffer gas, argon. If the entire driven section is filled with the test sample, the sample beyond the contact surface would not get heated by the reflected shock wave as it is already got attenuated by the expansion fan at the contact surface. Therefore, a small test section was made to carry out these experiments. In fact, this method was used extensively by various groups.[24–26] Three pressure transducers (PCB 113A22) were mounted towards the end of the driven section. The mounted pressure transducers were used to measure the shock velocity and thereby to calculate both the primary and reflected shock temperatures. The pressure transducer, which is mounted closest to the end flange, was used to record the pressure trace and the reaction time.

A typical pressure trace recorded using the pressure transducer mounted near the end flange is shown in figure 2. The reaction time of each experiment was measured from the pressure trace. Shock velocities were calculated using the time taken for the incident shock wave to travel between successive pressure transducers. The pressures behind the reflected shock waves

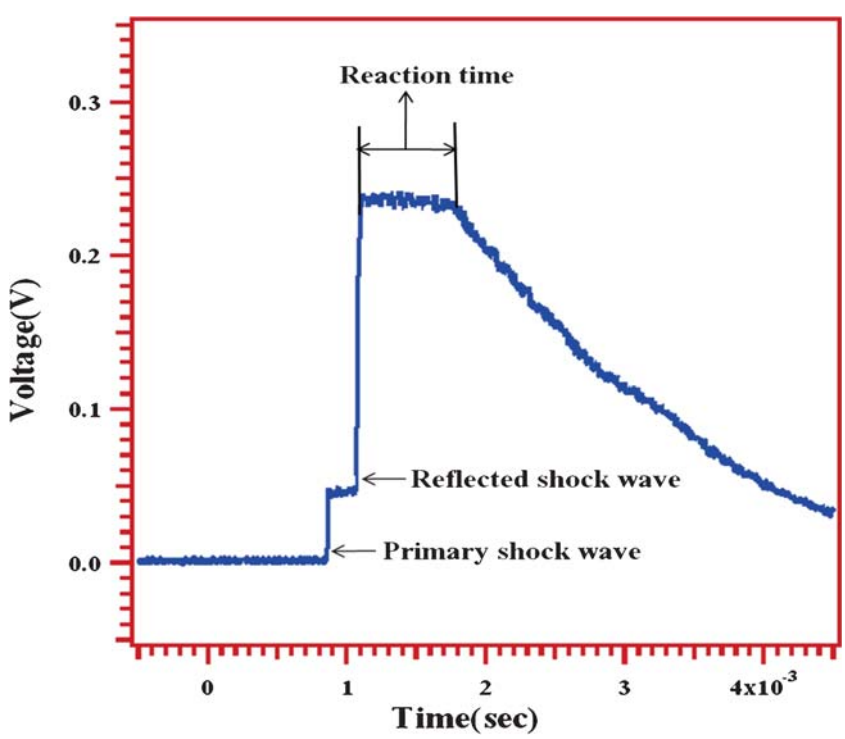

Figure 2. A typical pressure trace recorded by an oscilloscope showing the complete pressure profile in an experiment. The arrival of primary and reflected shock waves and reaction time are indicated on the pressure trace.

were calculated using the pressure jumps recorded in the pressure trace.

As described by many researchers earlier, the reflected shock temperature (T_5) computed by conventional Rankine-Hugoniot (R-H) relations[27] is given below. They suffer from real gas effects and boundary layer problems.[28–31]

$$\frac{T_5}{T_1} = \frac{\left\{2\left(\gamma_1 - 1\right) M_1^2 + \left(3 - \gamma_1\right)\right\}\left\{\left(3\gamma_1 - 1\right) M_1^2 - 2\left(\gamma_1 - 1\right)\right\}}{\left(\gamma_1 + 1\right)^2 M_1^2} \tag{1}$$

Where T_1 is the room temperature, T_5 is the reflected shock temperature, γ_1 is the specific heat ratio of the test gas and M_1 is the shock Mach number. To overcome the effects like real gas and boundary layer effects, chemists have developed the chemical thermometry method[32–35] to get the accurate reflected shock temperatures. In kinetics, as the accuracy in measuring the temperature is very important, the chemical thermometric method was used in our investigations. In the present investigation, the reflected shock temperatures were determined by the extent of reverse Diels-Alder decomposition of cyclohexeneto 1,3-butadiene and ethylene, which is added in the reaction mixture to serve as chemical thermometer.

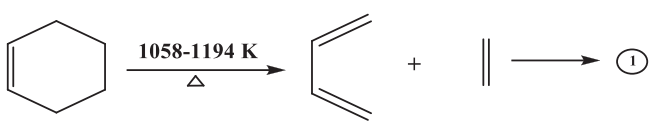

Recently, there was a revisit on the rate coefficient for the decomposition of the cyclohexene by Ronald Hanson's group for the reaction of cyclohexene → ethylene + 1,3-butadiene.[36] We have used this rate coefficient $k = 4.84 \times 10^{14} \exp\left(-63.39\,\text{kcal mol}^{-1}/\text{RT}\right)\ \text{s}^{-1}$, (where R is expressed in the units of kcal K^{-1} mol^{-1}) in the calculation of the reflected shock temperature. The accuracy of the temperatures estimated using the internal standard depends on the error associated with the reported rate coefficient for the decomposition of the internal standard. The reflected shock temperatures were calculated from the relation

$$T = -\left(E_a/R\right) / \left[ln\left\{-\frac{1}{At} ln\left(1 - \chi\right)\right\}\right]. \tag{2}$$

where 't' is the reaction time, 'A' and 'E_a' are the pre-exponential factor and activation energy of the reaction, and χ is the extent of reaction defined by $\chi = [\text{product}]_t/([\text{reactant}]_t + [\text{product}]_t)$.

Internal standard (ISD) method removes all the natural uncertainties in the physical properties. The introduction of the internal standard eliminates the uncertainty in the measurement of the temperature, because both the internal standard and reactant molecule experience the same reaction conditions. Therefore, these temperatures were used in the present investigation.

The driver and driven sections of the shock tube were separated by a pre-scored aluminum diaphragm of desired thickness. Before the experiment both the driver and driven sections were pumped down to approximately 1×10^{-6} Torr using a diffusion pump, after making the shock tube rich in argon environment. This procedure was repeated for two to three times before each experiment is carried out to ensure that no oxygen is left in the shock tube. 10 Torr of TMS and 10 Torr of cyclohexene were added into the sample section of the shock tube using a capacitance manometer (MKS 626B) and the mixture was diluted with argon till desired pressure (200-550 Torr) is attained. Argon alone was filled into the section between the sample compartment and the diaphragm. The pressure in the sample compartment was kept lower than the section between the sample compartment and aluminum diaphragm, by about 10 Torr to make sure the sample does not get diffused backwards, when the ball valve is opened before the experiment is carried out. The P_1 value of each experiment and initial concentrations of both the reactant and the internal standard are given in table 1. When P_1 is low, higher Mach number could be expected and a higher T_5 will be obtained. However, this generalized observation depends on other factors as well. P_4 plays a very significant role in achieving a targeted T_5, which in turn depends on the thickness of the diaphragm and the depth to which it was scored. Therefore, P_1 and P_4 plays a combined role on T_5. In the present experiment, the diaphragms used were scored to a depth of 20%, 25% and 30% of their thickness. As it is a combination of all these factors, it is difficult to talk about the attained T_5 by looking at P_1 alone.There will not be any significant or measurable changes in the reflected shock temperatures during the course of reaction, as the concentrations of the test samples are very less. The shock waves were generated by rupturing the diaphragm via filling the driver section with helium to the threshold pressure of the pre-scored aluminum diaphragm. After finishing the experiment, the post shocked mixtures were allowed to mix thoroughly for about 30 min. The post-shock mixtures were quantitatively analysed by gas chromatography (Agilent 6890 N). The samples were withdrawn from the shock tube and a constant volume of 0.5 mL samples were injected through an online gas sampling valve into the gas chromatograph equipped with a Flame Ionization Detector (FID). A Porapak-Q column was used for the analysis and oven temperature was programmed from 75°C to 180°C. Nitrogen was

Table 1. Experimental conditions and distribution of normalized concentrations of reactant and reaction products in the decomposition of TMS.

Sl. No	Pressure P_1 (Torr)	Initial concentration of TMS	Initial concentration of cyclohexene	T_5 (K)	P_5 (atm)	Reaction time (μs)	$[CH_4]_t/[TMS]_0$	$[C_2H_4]_t/[TMS]_0$	$[C_2H_6]_t/[TMS]_0$	$[C_3H_6]_t/[TMS]_0$	$[TMS]_t/[TMS]_0$
1	400	0.025	0.025	1058	14.7	544	0.0311	0.0211	0.0026	0.0038	0.941
2	500	0.020	0.020	1061	16.5	328	0.0292	0.0123	0.0017	0.0032	0.954
3	205	0.048	0.048	1063	14.9	330	0.0292	0.0123	0.0017	0.0032	0.954
4	525	0.019	0.019	1065	16.4	435	0.0118	0.0161	0.0039	0.0052	0.963
5	530	0.019	0.019	1066	15.6	445	0.0131	0.0160	0.0039	0.0052	0.962
6	450	0.022	0.022	1074	16.6	476	0.0606	0.0358	0.0072	0.0070	0.889
7	550	0.018	0.018	1084	13.8	470	0.0790	0.0523	0.0088	0.0065	0.853
8	550	0.018	0.018	1091	13.5	826	0.1671	0.2367	0.0135	0.0075	0.575
9	300	0.033	0.033	1096	13.9	600	0.1376	0.1338	0.0113	0.0071	0.710
10	350	0.029	0.029	1106	16.7	609	0.1735	0.1432	0.0126	0.0091	0.662
11	325	0.030	0.030	1108	14.9	620	0.1681	0.2504	0.0139	0.0075	0.560
12	350	0.029	0.029	1117	16.5	658	0.1751	0.2913	0.0116	0.0075	0.514
13	200	0.050	0.050	1118	12.2	868	0.2280	0.3818	0.0096	0.0065	0.374
14	325	0.030	0.030	1121	16.0	659	0.2140	0.3027	0.0140	0.0071	0.462
15	200	0.050	0.050	1122	10.6	766	0.1980	0.3479	0.0122	0.0070	0.435
16	275	0.036	0.036	1123	14.9	760	0.2496	0.3973	0.0083	0.0074	0.337
17	300	0.033	0.033	1124	14.4	590	0.1911	0.2688	0.0170	0.0079	0.515
18	300	0.033	0.033	1125	15.9	800	0.2293	0.3787	0.0099	0.0086	0.373
19	275	0.036	0.036	1126	15.2	752	0.2495	0.3627	0.0100	0.0090	0.369
20	275	0.036	0.036	1127	15.3	780	0.2571	0.3816	0.0106	0.0078	0.343
21	225	0.044	0.044	1129	13.6	844	0.2688	0.4002	0.0098	0.0081	0.313
22	250	0.040	0.040	1130	15.6	720	0.2637	0.3768	0.0096	0.0079	0.342
23	300	0.033	0.033	1131	16.0	790	0.2689	0.3911	0.0111	0.0085	0.320
24	250	0.040	0.040	1138	14.3	700	0.2457	0.4278	0.0090	0.0089	0.309
25	200	0.050	0.050	1141	13.1	830	0.2711	0.4314	0.0084	0.0077	0.281
26	225	0.044	0.044	1143	14.3	852	0.3085	0.4056	0.0101	0.0094	0.266
27	250	0.040	0.040	1151	14.0	710	0.2918	0.3856	0.0096	0.0072	0.306
28	200	0.050	0.050	1153	13.6	898	0.2945	0.4853	0.0077	0.0097	0.203
29	225	0.040	0.040	1162	13.8	838	0.2724	0.4605	0.0095	0.0067	0.251
30	200	0.050	0.050	1176	13.4	778	0.3422	0.4442	0.0111	0.0113	0.191
31	200	0.050	0.050	1179	13.9	778	0.3685	0.4771	0.0120	0.0122	0.130
32	325	0.030	0.030	1194	21.8	880	0.3766	0.4061	0.0078	0.0099	0.200
33	375	0.026	0.026	1194	22.8	870	0.4249	0.4739	0.0105	0.0090	0.082

used as a carrier gas in the analysis. The sensitivity of the flame ionization detector (FID) towards all the reactants and products were calibrated over a known range of concentrations. The concentration/mole fraction of left-out reactant and other products were calculated using the known sensitivity factors obtained in the calibration and the areas under each peak. A qualitative analysis was also carried out by using a Bruker's VERTEX 70 FTIR spectrometer.

2.1 *Materials and chemicals*

TMS (GC grade with >99% purity) and cyclohexene (reagent plus grade 99% purity) used in these experiments were purchased from Sigma Aldrich. TMS and cyclohexene were further purified by several cycles of freeze-pump-thaw method. Analysis of TMS and cyclohexene by gas chromatography showed no distinguishable impurities. Methane (99.5%), ethylene (99.5%), ethane (99.5%), propylene (99.5%), 1,3-butadiene (99.5%) and the high purity helium gas (99.995%) from Praxair Inc. were used as such in our experiments.

3. Results and Discussion

To understand the distribution of reaction products, 33 experiments were carried out with gas mixtures containing 10 Torr of TMS and 10 Torr of cyclohexene in argon as described in the experimental section, covering the temperature range of 1058–1194 K. Typical reaction times were 330–1000 μs and the pressure was

varied between 11 and 23 atm. Detailed conditions of each experiment and the normalized yields of products are given in table 1. The detectable products observed in the decomposition of TMS are methane (CH_4), ethylene (C_2H_4), ethane (C_2H_6) and propylene (C_3H_6). A gas chromatogram of a post shock mixture of TMS decomposed at 1151 K is shown in figure 3. The concentration ratios of 1,3-butadiene and cyclohexene were used to determine the reflected shock temperature. In these experiments, ethylene is the product of both the reactant TMS and internal standard. This was confirmed by decomposing TMS alone behind the reflected shock waves in the studied temperature range and ethylene was observed to be one of the products listed before. The contributions of cyclohexene towards the total concentration of ethylene was computed by measuring the concentration of 1,3-butadiene, which was formed in equal concentrations via reaction 1. It was further confirmed that, 1,3-butadiene does not decompose in the investigated range of the temperatures, by carrying out its decomposition independently. Skinner *et al.*,[37] and Hidaka *et al.*,[38] also have reported that 1,3-butadiene does not decompose in this temperature range. Therefore, we have subtracted the yield of ethylene due to the decomposition of cyclohexene, which is essentially equal to the concentration of 1,3-butadiene from the total yield of ethylene, to get the ethylene yield due to the decomposition of TMS alone.

We have carried out FTIR analysis, to find out the silicon containing species and hydrocarbons. A FTIR spectrum of the post shock mixture of TMS in argon, decomposed at 1179 K is shown in figure 4. The Si-CH_3 group is easily recognized with a sharp peak at 1260 cm^{-1}, and the peaks around 1447 and 947 cm^{-1} indicate the presence of olefins. The peak at 2964 cm^{-1} shows the presence of hydrocarbons.

The decay of the reactant and formation of products are shown as a function of temperature in figure 5. Concentrations of products methane and ethylene are observed to be continuously increasing with the temperature. The ethane concentration was observed to be increasing up to ≈1150 K and then decreasing due to several other reactions. Propylene concentrations seem to be increasing upto 1120 K and then more or less constant thereafter.

The rate coefficients for the decomposition of TMS were calculated by using the following equation

$$k_{total} = -\ln\{[TMS]_t/[TMS]_0\}/t \qquad (3)$$

where $[TMS]_t$ and $[TMS]_0$ are the experimentally quantified concentration of TMS at the end of the reaction time 't' and initial concentration respectively. The obtained rate coefficients were used to plot the Arrhenius equation and are shown in figure 6. The rate coefficients are observed to be non-linear across the studied temperature range. Therefore, the data were fit to the Arrhenius equation in two different temperature ranges i.e., 1058-1130K and 1130-1194K using linear least squares method. The temperature dependent

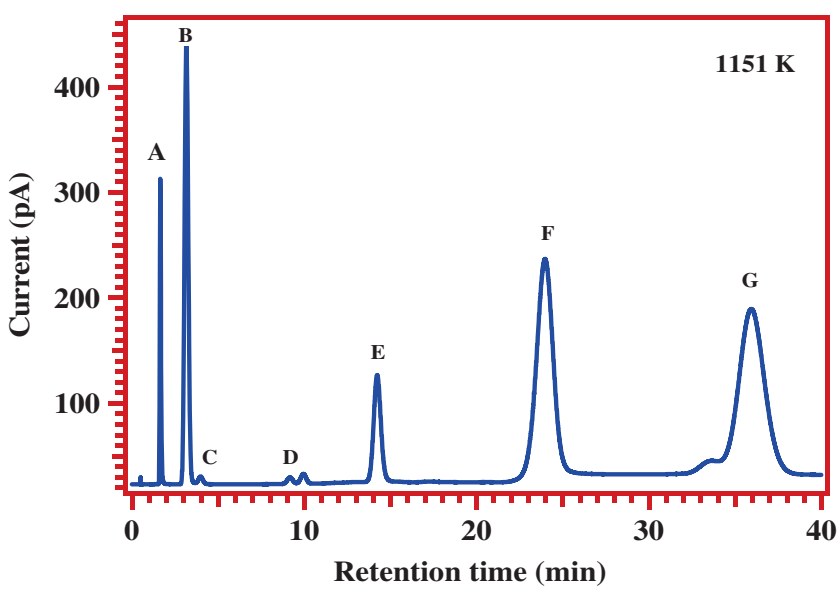

Figure 3. Gas chromatogram showing the products of the post shock mixture of the experiment carried out at 1151 K. The peaks labeled in the chromatogram are **(A)** methane, **(B)** ethylene, **(C)** ethane, **(D)** propylene, **(E)** 1,3-butadiene, **(F)** tetramethylsilane and **(G)** cyclohexene.

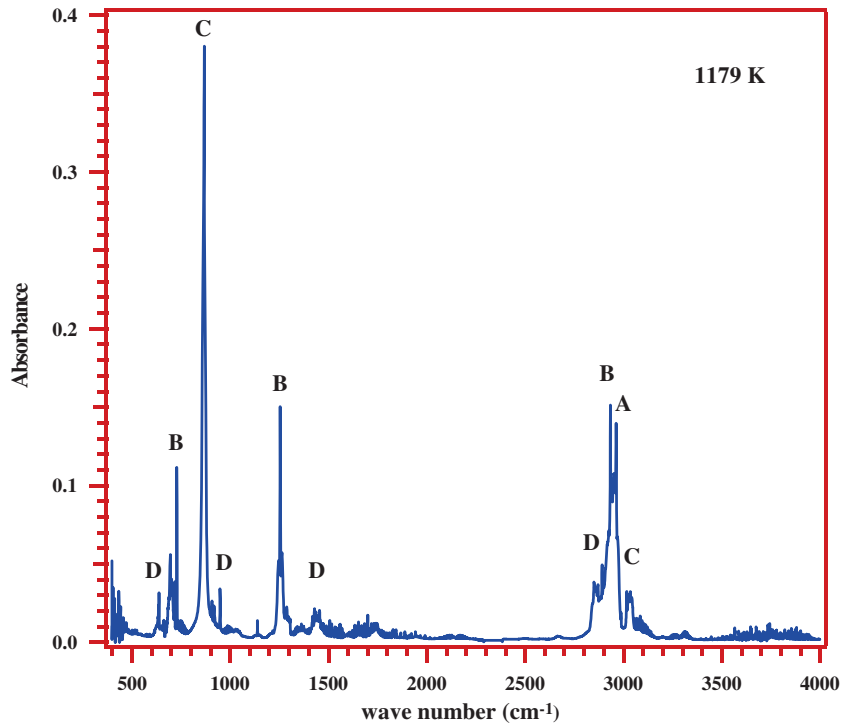

Figure 4. FT-IR spectrum of the post shock mixture of tetramethylsilane diluted in argon when the experiment was carried out at 1179 K. The peaks labeled in the spectrum are **(A)** methane, **(B)** tetramethylsilane, **(C)** ethylene, and **(D)** propylene.

rate coefficients obtained are k_{total} (1058–1130 K) = $(4.61 \pm 0.70) \times 10^{18} \exp(-(79.9\,\text{kcal mol}^{-1} \pm 3.5)/RT)\ \text{s}^{-1}$, k_{total} (1130–1194 K) = $(1.33 \pm 0.19) \times 10^{6} \exp(-(15.3\,\text{kcal mol}^{-1} \pm 3.5)/RT)\ \text{s}^{-1}$ where, R is expressed in the units of kcal $K^{-1}\,\text{mol}^{-1}$. The errors reported here are the errors obtained in the linear least squares fit of the data. The nonlinearity in the Arrhenius plot is due to many reaction channels in the decomposition process of TMS. At high temperature region TMS undergo unimolecular dissociation as well as bimolecular reactions[45,46] ($CH_3 + (CH_3)_4Si \rightarrow CH_4 + (CH_3)_3SiCH_2$, $(CH_3)_4Si + H \rightarrow H_2 + (CH_3)_3SiCH_2$). As the consumption of the reactant is because of both the competitive or parallel reactions, the Arrhenius plot is expected to be non-linear, which is the case as well. In addition, the products ethane and propylene were observed to be increasing upto 1125K and then start decreasing as they get dissociated into other products, which may be one of the reasons for sudden deviation in the Arrhenius plot. The measured rate coefficient of reaction R1 from the present experiments is mostly valid in the temperature range of 1058–1194 K only. Even within the studied temperature range the trends are different between 1058–1130 K and 1130–1194 K (figure 6). Therefore, the extrapolation may not be valid.

The rate coefficients for the formation of methane were computed by using the following relation[39]

$$k_{\text{methane}} = \frac{[\text{Methane}]_t}{[TMS]_0 - [TMS]_t} \times k \text{ total.} \qquad (4)$$

where $[\text{Methane}]_t$ is the concentration of methane at the end of reaction time 't'. The experimentally obtained rate coefficients were used to plot the Arrhenius equation and are shown in figure 7. The data were fit using linear least squares method and the temperature dependent rate coefficient for the formation of methane was obtained to be k_{methane} (1058–1194 K) = $(4.36 \pm 1.23) \times 10^{14} \exp(-(61.9\,\text{kcal mol}^{-1} \pm 4.9)/RT)\ \text{s}^{-1}$. The activation energy for the formation of methane is determined to be 62.0 kcal mol^{-1}, which is about 6kcal mol^{-1} lower than the value reported by Clifford *et al.*,[19] As mentioned in the introduction, Baldwin *et al.*,[20] have reported two rate expressions for the two different range of temperatures. The activation energy obtained in our experiments is 4.5 kcal mol^{-1} higher than the one reported by Baldwin *et al.*,[20] in the temperature range of 840–950 K. However, it is 23 kcal mol^{-1} lower than the activation energy reported in the temperature range of 955–1055 K. The value of rate coefficient for the formation of methane obtained in the present work at

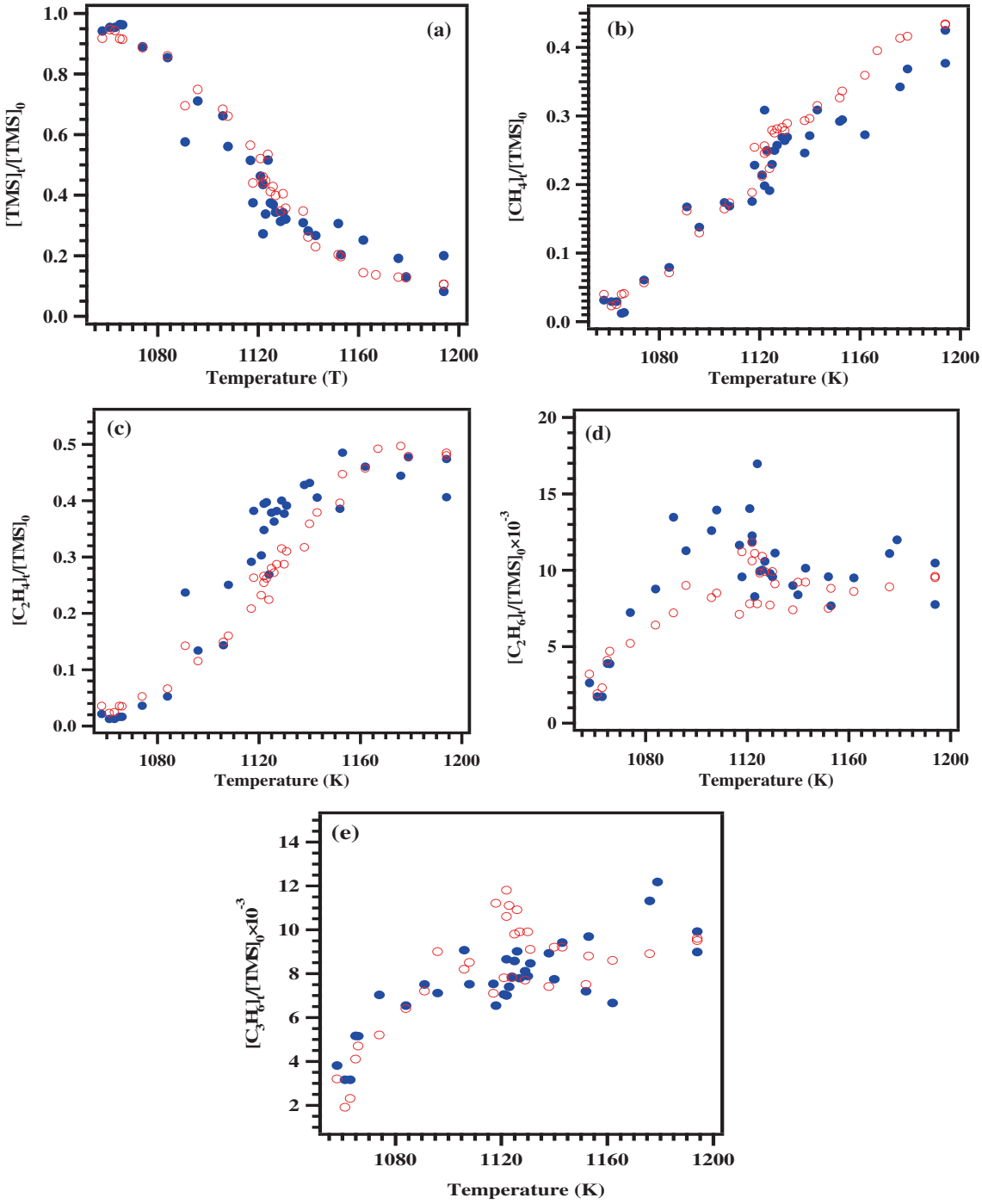

Figure 5. The complete decomposition profile of TMS behind the reflected shock waves and the profiles of the products obtained in the temperature range of 1058–1194 K. The filled symbols correspond to the experimental yields and open symbols correspond to the simulated data. The plots labeled are **(a)** tetramethylsilane **(b)** methane **(c)** ethylene **(d)** ethane and **(e)** propylene.

1058 K is almost two orders of magnitude higher than that reported at 1055 K. The rate coefficients reported in earlier investigation were obtained using pulsed stirred flow reactor wherein the reaction times were varied between 13 and 120 s. The secondary chemistry and the wall effects will definitely be significant in their studies for such long reaction times. However, in the present experiments, the reaction time was a maximum of 1 ms. One of the advantages of using the SPST technique is that the wall effects are almost negligible in such short durations. This could be one of the reasons for such a difference in rate coefficients. In addition, many other experimental uncertainties could also contribute.

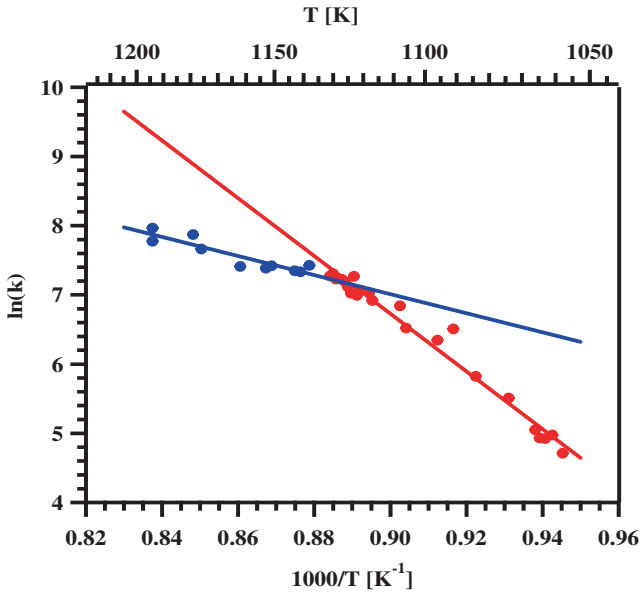

Figure 6. Arrhenius plot for the overall decomposition of TMS in the temperature range of 1058–1194 K. The rate coefficients were calculated using the equation $k_{total} = -\frac{\ln\{[TMS]_t/[TMS]_0\}}{t}$. The obtained temperature dependent rate coefficients for two different temperature ranges are k_{total} (1058–1130 K) = (4.61 ± 0.70) $\times 10^{18}$ exp (−(79.9 kcal mol^{-1} ± 3.5)/RT) s^{-1}, k_{total} (1130–1194 K) = (1.33 ± 0.19) $\times 10^{6}$exp (−(15.3 kcal mol^{-1}± 3.5)/RT) s^{-1}.

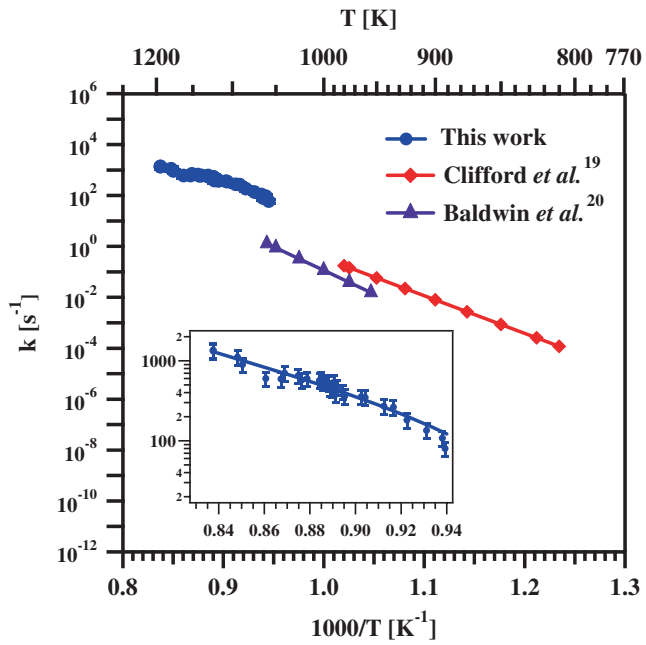

Figure 7. Arrhenius plot for the formation of methane in the decomposition of TMS. The obtained temperature dependent rate coefficient for the entire experimental temperature range is $k_{methane}$ = (4.36 ± 9.72) $\times 10^{14}$ exp (−(61.9 kcal mol^{-1} ± 4.9)/RT) s^{-1}. The insert is the zoom of the data obtained in the present experiments.

The formation of Si-C cannot be understood by this study because SiC growth was not focused in the present investigation. Various studies are available on the pyrolysis of neopentane in literature.[40–43] The available studies report that the primary dissociation of neopentane also happens via C-C (Si-C bond cleavage in TMS) bond cleavage by forming methyl and tert-butyl radicals. Taylor *et al.*,[41] studied in detail on the homogeneous gas phase pyrolysis of neopentane using a reactor in the temperature range of 920–1070 K. The reaction products observed on pyrolysis of neopentane are hydrogen, methane, ethane, ethylene, propylene, allene, methylacetylene, 2-methyl-l-butene, 2-methyl-2-butene, isoprene and isobutylene. The initial rate-determining reaction is the unimolecular decomposition of neopentane to form t-butyl and methyl radicals. Hydrogen, ethane and methane appear to form by radical combinations, which is also the case in the present study. In the decomposition of neopentane, the formation of methane happens *via* hydrogen abstraction from the reactant by CH_3 radicals; isobutylene is formed by decomposition of the t-butyl radical; ethylene, propylene, and allene are formed by degradation of isobutylene; and the other products by a variety of reactions. The formation of methane in the decomposition of TMS happen *via* the same mechanism. i.e., abstraction of hydrogen from the reactant by CH_3 radicals. The temperature dependent rate coefficients for the overall decomposition of TMS and neopentane are given in table 2 for the ready comparison. The activation energies for the overall decomposition of TMS and neopentane are just same (80 kcal mol^{-1}) in the temperature range of 1000–1100 K. This could be the obvious reason for the similar mechanism between TMS and neopentane.

3.1 *Kinetic simulations*

To understand the reaction mechanism in the decomposition of TMS, a reaction kinetic scheme is proposed with 21 reaction species and 38 elementary reactions. The proposed reaction scheme is given in table 3. The reaction mechanism proposed earlier[19–21] was also included in the present kinetic scheme. The rate coefficients for all the proposed reactions except for R1 were taken from the literature.[46–71] The rate coefficient obtained for the formation of methane (R1) in the present investigation was used in the simulations. The rate coefficients for the proposed reactions are given in k = A exp(-E_a/RT) or k = AT^nexp(-E_a/RT) formats, where A factors are given in s^{-1} and cm^3 mol^{-1}s^{-1} for first and second order reactions respectively, and

Table 2. The comparison of temperature dependent rate coefficients for total decomposition of TMS in the present investigation and earlier studies on neopentane.

Total decomposition of TMS			Total decomposition of neopentane		
Temperature (K)	A (s^{-1})	E_a (kcal mol^{-1})	Temperature (K)	A (s^{-1})	E_a (kcal mol^{-1})
1058–1130 K[a]	$(4.61 \pm 0.70) \times 10^{18}$[a]	79.9[a]	920–1070 K[41]	7.94×10^{16}[41]	80.5[41]
1130–1194 K[b]	$(1.33 \pm 0.19) \times 10^{6}$[b]	15.3[b]	1260–1462 K[42]	8.66×10^{12}[42]	60.5[42]
			793–953 K[43]	5.01×10^{17}[43]	85.1[43]

[a]Total decomposition of TMS at 1058–1130 K in present study, [b]Total decomposition of TMS at 1130-1149K in present study,[41] Taylor *et al.*,[42] Sivaramakrishnan *et al.*,[43] Pacey.

Table 3. Proposed reaction scheme for the decomposition of TMS with 21 reaction species and 38 elementary reactions.[a]

No	Reaction	A	n	E_a	Reference
R1	$(CH_3)_4Si \rightarrow CH_3 + (CH_3)_3Si$	4.36×10^{14}	0.00	61.98	This work
R2	$CH_3 + (CH_3)_4Si \rightarrow CH_4 + (CH_3)_3SiCH_2$	1.99×10^{11}	0.00	9.60	45
R3	$(CH_3)_3SiCH_2 \rightarrow CH_3 + (CH_3)_2SiCH_2$	1.00×10^{15}	0.00	50.66	20
R4	$(CH_3)_4Si + H \rightarrow H_2 + (CH_3)_3SiCH_2$	4.71×10^{5}	2.65	4.88	46
R5	$(CH_3)_3Si \rightarrow (CH_3)_2Si + CH_3$	1.00×10^{15}	0.00	52.80	20
R6	$CH_3 + CH_3 \rightarrow C_2H_6$	4.47×10^{13}	−0.69	0.17	47
R7	$(CH_3)_2Si \rightarrow CH_3Si + CH_3$	1.00×10^{15}	0.00	52.80	20
R8	$CH_3 + CH_3 \rightarrow C_2H_5 + H$	2.40×10^{13}	0.00	12.88	48
R9	$CH_3 + CH_3 \rightarrow C_2H_4 + H_2$	9.90×10^{15}	0.00	32.98	49
R10	$C_2H_5 + H \rightarrow C_2H_4 + H_2$	1.81×10^{14}	0.00	0.00	50
R11	$C_2H_6 + CH_3 \rightarrow C_2H_5 + CH_4$	3.02×10^{12}	0.00	13.59	51
R12	$C_2H_5 \rightarrow C_2H_4 + H$	3.06×10^{10}	0.95	36.94	52
R13	$C_2H_5 + C_2H_5 \rightarrow C_2H_4 + C_2H_6$	1.45×10^{12}	0.00	0.00	53
R14	$H_2 + Ar \rightarrow H + H + Ar$	5.33×10^{14}	0.00	96.01	54
R15	$C_2H_4 + CH_3 \rightarrow C_3H_6 + H$	2.00×10^{13}	0.00	10.00	50
R16	$C_3H_6 + H \rightarrow C_2H_4 + CH_3$	1.32×10^{12}	1.50	2.01	55
R17	$CH_4 \rightarrow CH_3 + H$	7.80×10^{14}	0.00	103.83	50
R18	$CH_4 + CH_3 \rightarrow C_2H_6 + H$	2.98×10^{11}	1.00	44.91	56
R19	$C_3H_6 \rightarrow CH_3 + C_2H_3$	8.00×10^{14}	0.00	88.03	55
R20	$C_2H_5 + H \rightarrow C_2H_6$	4.50×10^{13}	0.00	0.00	57
R21	$C_2H_3 + H_2 \rightarrow C_2H_4 + H$	2.04×10^{14}	2.56	5.03	58
R22	$CH_3 + Ar \rightarrow CH_2 + H + Ar$	2.82×10^{15}	0.00	84.56	59
R23	$CH_3 + H \rightarrow CH_2 + H_2$	6.02×10^{13}	0.00	15.10	53
R24	$CH_3 + CH_2 \rightarrow C_2H_4 + H$	6.02×10^{13}	0.00	0.00	60
R25	$CH_2 + H \rightarrow CH + H_2$	1.63×10^{14}	0.00	0.00	61
R26	$CH_3 + CH \rightarrow C_2H_3 + H$	3.00×10^{13}	0.00	0.00	62
R27	$CH_3 + Ar \rightarrow CH + H_2 + Ar$	6.90×10^{14}	0.00	82.50	63
R28	$CH_4 + H \rightarrow CH_3 + H_2$	1.77×10^{14}	0.00	13.78	63
R29	$C_2H_4 + C_2H_5 \rightarrow C_2H_6 + C_2H_3$	1.58×10^{11}	0.00	14.86	64
R30	$CH_4 + H \rightarrow CH_3 + 2\,H$	$4.40 \times 10^{\circ}$	0.00	7.88	65
R31	$C_2H_5 + C_3H_6 \rightarrow C_2H_6 + n\text{-}C_3H_5$	6.92×10^{10}	0.00	5.19	66
R32	$C_3H_6 + H \rightarrow n\text{-}C_3H_7$	2.50×10^{11}	0.51	2.62	67
R33	$C_3H_6 + H \rightarrow iso\text{-}C_3H_7$	4.24×10^{11}	0.51	1.23	67
R34	$iso\text{-}C_3H_7 \rightarrow C_2H_4 + CH_3$	1.00×10^{12}	0.00	34.58	68
R35	$iso\text{-}C_3H_7 + C_2H_5 \rightarrow C_2H_6 + C_3H_6$	3.13×10^{10}	−0.35	0.00	69
R36	$n\text{-}C_3H_7 \rightarrow C_2H_4 + CH_3$	2.70×10^{13}	0.00	30.04	70
R37	$n\text{-}C_3H_7 + C_2H_5 \rightarrow C_2H_6 + C_3H_6$	1.45×10^{12}	0.00	0.00	69
R38	$n\text{-}C_3H_5 + H_2 \rightarrow C_3H_6 + H$	6.90×10^{14}	2.38	82.50	71

[a]Rate expressions are given in the form of $k = A \exp(-E_a/RT)$ and $k = AT^n \exp(-E_a/RT)$. The units of the rate coefficients are s^{-1} and $cm^3\,mol^{-1}s^{-1}$ for first and second order reactions, respectively. The units for the activation barrier are kcal mol^{-1}.

activation energies are given in kcal mol^{-1}. Kinetic simulations were carried out at experimentally determined temperatures and reaction times. All simulations were carried out using IBM's chemical kinetic simulator.[44] The agreement between the simulated concentrations and the experimentally determined concentrations of TMS and the major products *viz*. CH_4 and C_2H_4 is very good. In case of minor products C_2H_6 and C_3H_6, the agreement seems to be reasonably good. It should be noted here that, the maximum concentrations of these minor products are less than 2% in the temperature range used in this study.

The reaction mechanism suggested[19,20] in the previous studies for decomposition of TMS was confined to lower temperatures (840–1055 K). However, kinetic simulations were not carried out in their studies to reproduce experimental concentrations of reactant and products. In the present work, detailed chemical kinetic mechanism for TMS decomposition was proposed. The present reaction scheme was able to simulate the experimental concentrations of reactant and products in the temperature range of 1058–1194 K. The proposed mechanism in the present studies explains the formation of all the products quantitatively.

3.1a *Methane*: The formation of CH_4 from the reactant TMS can be explained by the formation of CH_3 radicals and trimethylsilyl radicals ($(CH_3)_3Si$) via Si-C bond cleavage. Each of these two radicals CH_3 and $(CH_3)_3Si$ further participate in secondary reactions via abstraction, recombination and dissociation reactions. The competition between these three classes of elementary reactions determines the concentrations of all the reaction products in the decomposition of TMS. The $(CH_3)_3Si$, and $(CH_3)_2Si$ radicals further undergo decomposition through Si-C bond cleavage to produce CH_3 radicals, dimethylsilyl ($(CH_3)_2Si$) and methylsilyl ($(CH_3)Si$) radicals respectively.

$$(CH_3)_4Si \rightarrow CH_3 + (CH_3)_3Si \; k_1 = 4.36 \times 10^{14} \exp(-61.98/RT) \; s^{-1} \quad (R1)$$

$$(CH_3)_3Si \rightarrow (CH_3)_2Si + CH_3 k_5 = 1.00 \times 10^{15} \exp(-52.80/RT) \; s^{-1} \quad (R5)$$

Studies by Clifford *et al*.,[19] and Baldwin *et al*.,[20] show that the first order rate coefficient for the formation of methane at high temperatures is a non-chain process and rate coefficient is determined by reaction R1. The CH_3 radicals thus formed in turn abstract any one of the H atom present in any one of the CH_3 groups in TMSin the reaction mixture to produce CH_4. Thekinetic parameters for this reactionwere reported by Baldwin *et al.*,[20]

$$CH_3 + (CH_3)_4Si \rightarrow CH_4 + (CH_3)_3SiCH_2 k_2 = 1.99 \times 10^{11} \exp(-9.60/RT) \; cm^3 mol^{-1} s^{-1} \quad (R2)$$

The reaction between CH_3 and C_2H_6 to form CH_4 cannot be ruled out and therefore a reaction R11 to this effect is added to the scheme.

$$C_2H_6 + CH_3 \rightarrow C_2H_5 + CH_4 k_{11} = 3.02 \times 10^{12} \exp(-13.59/RT) \; cm^3 mol^{-1} s^{-1} \quad (R11)$$

Although dissociation of methane in the studied temperature range is negligible, we cannot rule out the formation of CH_3 radicals via CH_4 dissociation. Therefore, a reaction R17 is added in the reaction scheme.

$$CH_4 \rightarrow CH_3 + H k_{17} = 7.80 \times 10^{14} \exp(-103.83/RT) s^{-1} \quad (R17)$$

It is obvious that R17 is highly insensitive and it is also reflected in the sensitivity analysis. Loss of CH_4 via its reaction with H atom (R28 and R30) are also included in the proposed reaction scheme for completeness.

$$CH_4 + H \rightarrow CH_3 + H_2 k_{28} = 1.77 \times 10^{14} \exp(-13.78/RT) cm^3 mol^{-1} s^{-1} \quad (R28)$$

$$CH_4 + H \rightarrow CH_3 + 2H k_{30} = 0.44 \times 10^{1} \exp(-7.88/RT) \; cm^3 mol^{-1} s^{-1} \quad (R30)$$

The sensitivity of each reaction towards the formation and decomposition of CH_4 was carried out by varying the rate coefficients of each reaction by a factor of 10. The results are shown in figure 8 in terms of percentage change in the concentrations with respect to the reaction numbers. It is obvious from this Figure that the reactions R1 and R5 are very sensitive to the formation of CH_4. In both these reaction paths CH_3 radical is formed which is the key species for the decomposition of TMS. Reactions R12, R13, R30 and R38 have shown significant influence on the formation of methane.

3.1b *Ethylene*: The other major product is ethylene, which is formed mainly via decomposition of ethyl radical (C_2H_5). Concentrations of C_2H_4 were found to be higher than the concentrations of CH_4 by 10% in the studied temperature range. The major source for the formation of C_2H_5 radical is the self-reaction of CH_3 radicals (R8).

$$CH_3 + CH_3 \rightarrow C_2H_5 + H k_8 2.40 \times 10^{13} \exp(-12.88/RT) \; cm^3 mol^{-1} s^{-1} \quad (R8)$$

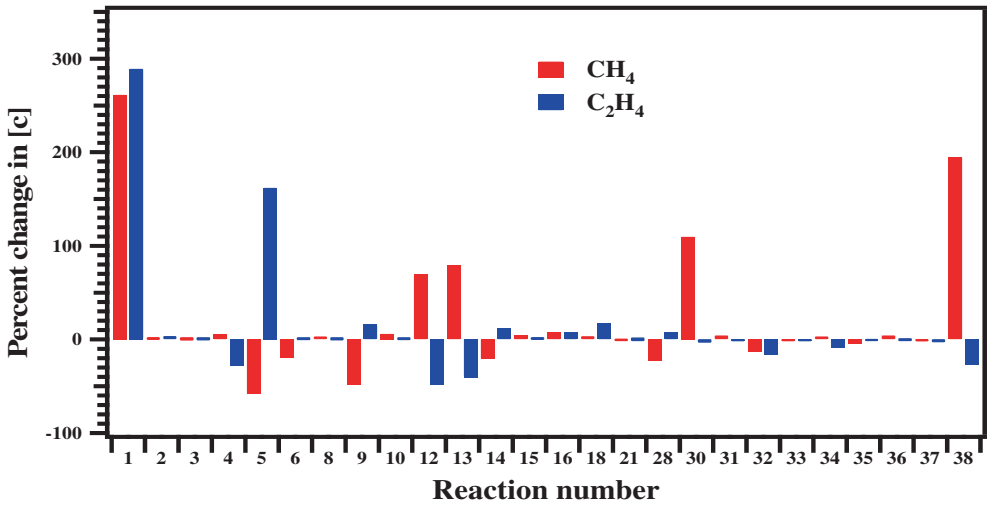

Figure 8. Sensitivity analysis of the proposed reaction scheme carried out at 1141 K for the formation of methane and ethylene. The rate coefficients were varied by a factor of 10 to see the sensitivity of each reaction for the formation of methane and ethylene.

It should also be noted here that the self-reaction of CH_3 radical also form C_2H_4 directly (R9).

$$CH_3 + CH_3 \rightarrow C_2H_4 + H_2 k_9 = 9.90 \times 10^{15} \exp(-32.98/RT)\ cm^3 mol^{-1} s^{-1} \quad (R9)$$

C_2H_4 is also formed via the reaction of C_2H_5 with H atom (R10) in the decomposition of TMS.

$$C_2H_5 + H \rightarrow C_2H_4 + H_2 k_{10} = 1.81 \times 10^{14} cm^3 mol^{-1} s^{-1} \quad (R10)$$

The C_2H_5 radical undergo unimolecular decomposition (R12) to form C_2H_4 and H atoms. The reaction of C_2H_5 radical with another C_2H_5 radical (R13) leads to the formation of C_2H_4, in addition to C_2H_6. These reactions are the major contributors to the formation of C_2H_4.

$$C_2H_5 \rightarrow C_2H_4 + Hk_{12} = 3.06 \times 10^{10} (T)^{0.95} \exp(-36.94/RT)\ s^{-1} \quad (R12)$$

$$C_2H_5 + C_2H_5 \rightarrow C_2H_4 + C_2H_6 k_{13} = 1.45 \times 10^{12}\ cm^3\ mol^{-1} s^{-1} \quad (R13)$$

As propylene is one of the minor products, formation of C_2H_3 radical (R19) is included in the reaction scheme. Also, a bimolecular reaction of CH_3 with the buffer gas (Ar) will lead to the formation of CH_2 (carbene) intermediate and this reaction is included in the reaction scheme. The C_2H_3 radical further reacts with H_2 (R21) and CH_2 (R24) to form C_2H_4 and these two reactions are the minor contributors to the formation of C_2H_4.

$$C_2H_3 + H_2 \rightarrow C_2H_4 + Hk_{21} = 2.04 \times 10^{14} (T)^{2.56} \exp(-5.03/RT)\ cm^3\ mol^{-1} s^{-1} \quad (R21)$$

$$CH_3 + CH_2 \rightarrow C_2H_4 + Hk_{24} = 6.02 \times 10^{13} cm^3 mol^{-1} s^{-1} \quad (R24)$$

Propylene reacts with H atoms to form both n-C_3H_7 and iso-C_3H_7 radicals (R37 & R38), respectively. These two radicals further decompose (R34 & R36) to give C_2H_4. As the concentrations of both propylene and the subsequently formed radicals are minimum in the decomposition reaction of TMS, the contributions of these reactions may be negligible.

$$\text{iso-}C_3H_7 \rightarrow C_2H_4 + CH_3 k_{34} = 1.00 \times 10^{12} \exp(-34.58/RT)\ s^{-1} \quad (R34)$$

$$\text{n-}C_3H_7 \rightarrow C_2H_4 + CH_3 k_{36} = 2.70 \times 10^{13} \exp(-30.04/RT)\ s^{-1} \quad (R36)$$

The sensitivity analysis of the proposed reaction scheme is carried out for the formation of C_2H_4 and the results are shown in figure 8. Reactions R1 and R5 are very sensitive for the formation of C_2H_4 as the formation of CH_3 radicals governs the formation of C_2H_5 radicals. Two more reactions which have shown influence on the formation of C_2H_4 are R12 and R13.

3.1c *Minor products*: The minor reaction products observed in the experiments are ethane (C_2H_6) and propylene (C_3H_6). The concentrations of these two products are less than 2%, when compared with the main products. The concentration of C_2H_6 was observed to be increasing upto 1120 K and beyond this temperature the concentrations of C_2H_6 were found to be decreasing. The major channel for the formation of C_2H_6 is the recombination of two CH_3 radicals (R6).

$$CH_3 + CH_3 \rightarrow C_2H_6 k_6 = 4.47 \times 10^{13} (T)^{-0.69} \exp(-0.17/RT)\ cm^3 mol^{-1} s^{-1} \quad (R6)$$

The minor channels for the formation of ethane include the abstraction of H atom by CH_3 radical from methane (R18), H atom abstraction reaction by C_2H_5 radical from ethylene (R29) and from propylene radical (R31), and the reaction of C_2H_5 radical with H atom (R20).

$$CH_4 + CH_3 \rightarrow C_2H_6 + H k_{18} = 2.98 \times 10^{11} (T)^{1.00} \exp(-44.91/RT) cm^3\, mol^{-1} s^{-1} \quad (R18)$$

$$C_2H_5 + H \rightarrow C_2H_6 k_{20} = 4.50 \times 10^{13} cm^3 mol^{-1} s^{-1} \quad (R20)$$

$$C_2H_4 + C_2H_5 \rightarrow C_2H_6 + C_2H_3 k_{29} = 1.58 \times 10^{11} \exp(-14.86/RT) cm^3\, mol^{-1} s^{-1} \quad (R29)$$

$$C_2H_5 + C_3H_6 \rightarrow C_2H_6 + n\text{-}C_3H_5 k_{31} = 6.92 \times 10^{10} \exp(-5.19/RT) cm^3 mol^{-1} s^{-1} \quad (R31)$$

The contribution of reactions of C_2H_5 radicals with both n-C_3H_7 and iso-C_3H_7 (R37 & R35) radicals was observed to be negligibly small during the simulations.

$$iso\text{-}C_3H_7 + C_2H_5 \rightarrow C_2H_6 + C_3H_6 k_{35} = 3.13 \times 10^{10} (T)^{-0.35} cm^3 mol^{-1} s^{-1} \quad (R35)$$

$$n\text{-}C_3H_7 + C_2H_5 \rightarrow C_2H_6 + C_3H_6 k_{37} = 1.45 \times 10^{12} cm^3 mol^{-1} s^{-1} \quad (R37)$$

The contribution of the reactions R6 and R18 depends on the availability of CH_3 radicals. It is obvious from the proposed scheme that CH_3 radicals are involved in many other reactions. Therefore, the availability of CH_3 radicals depends on the rates of other reactions. The concentrations of ethane formed in the simulations using the proposed scheme are in good agreement with experimentally measured concentrations.

Propylene is another minor product obtained in the experiments with a maximum concentration of 1%. Its formation is included in the reaction scheme by adding the reaction of CH_3 radicals with one of the major product, ethylene.

$$C_2H_4 + CH_3 \rightarrow C_3H_6 + H k_{15} = 2.0 \times 10^{13} \exp(-10.00\ kcal\, mol^{-1}/RT) cm^3 mol^{-1} s^{-1} \quad (R15)$$

Another reaction in which C_3H_6 is formed is the reaction of C_2H_5 radicals with both n-C_3H_7 and iso-C_3H_7 radicals (R37 & R35). As described earlier, the concentrations of n-C_3H_7 and iso-C_3H_7 radicals are very insignificant, these two reactions would not show any significant contribution in the formation of propylene. The propylene thus formed is consumed in its reactions with CH_3 radicals (R16) and H atom (R32 and R33). Propylene undergoes C-C bond scission in the studied temperature range to form CH_3 radicals. Therefore, reaction R19 is added in the proposed scheme.

$$C_3H_6 + H \rightarrow C_2H_4 + CH_3 k_{16} = 1.32 \times 10^{12} (T)^{1.50} \exp(-2.01/RT)\, cm^3 mol^{-1} s^{-1} \quad (R16)$$

$$C_3H_6 \rightarrow CH_3 + C_2H_3 k_{19} = 8.00 \times 10^{14} \exp(-88.03/RT) s^{-1} \quad (R19)$$

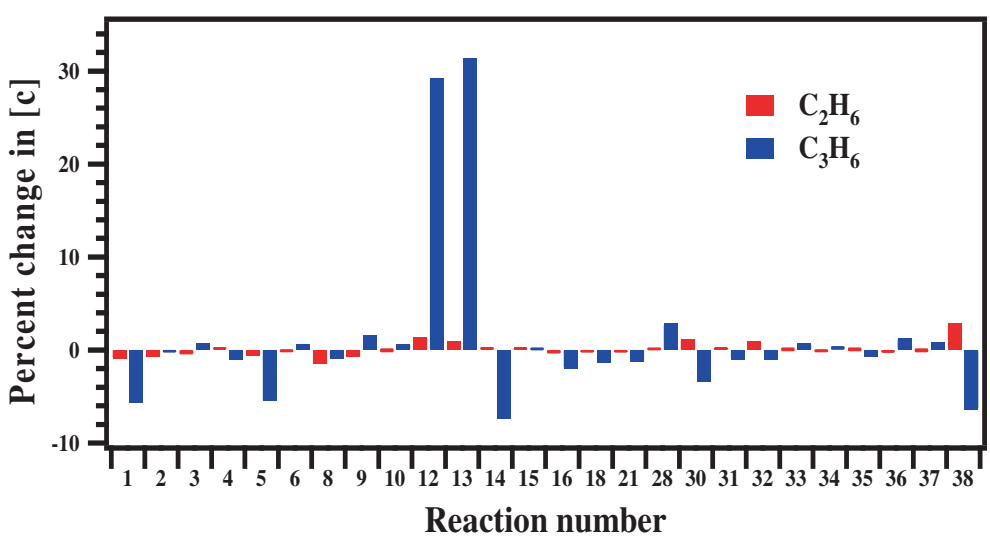

Figure 9. Sensitivity analysis of the proposed reaction scheme carried out at 1141 K for the formation of ethane and propylene. The rate coefficients were varied by a factor of 10 to see the sensitivity of each reaction for the formation of ethane and propylene.

$$C_3H_6 + H \rightarrow \text{n-}C_3H_7 k_{32} = 2.50 \times 10^{11}(T)^{0.51} \exp(-2.62/RT)\text{cm}^3\text{mol}^{-1}\text{s}^{-1} \quad \text{(R32)}$$

$$C_3H_6 + H \rightarrow \text{iso-}C_3H_7 k_{33} = 4.24 \times 10^{11}(T)^{0.51} \exp(-1.23/RT)\text{cm}^3\text{mol}^{-1}\text{s}^{-1} \quad \text{(R33)}$$

The concentrations of propylene predicted using the proposed reaction scheme is in reasonably good agreement with the experimentally measured concentrations of propylene.

The sensitivity analyses of the proposed reactions for the formation of both the minor products namely ethane and propylene were carried out and are shown in figure 9. No reaction was found to be significantly sensitive in case of either the formation or decomposition of ethane. However, in case of propylene, reactions R12 and R13 were found to be very sensitive. In both these reactions, the C_2H_5 radical is consumed. Therefore, it is obvious that the formation of propylene is governed by the available concentrations of C_2H_5 radicals.

Another very important product that we could not measure in the experiments is H_2. Both GC-FID and IR techniques are not suitable to identify this product. However, the proposed reaction scheme has predicted formation of significant amount of H_2. The contribution for the formation of H_2 is significant via the reactions R23 and R28, because the concentrations of CH_3 and TMS are high when compared to other radicals.

$$(CH_3)_4Si + H \rightarrow H_2 + (CH_3)_3SiCH_2 k_4 = 4.71 \times 10^5(T)^{2.65} \exp(-4.88/RT)\text{cm}^3\text{mol}^{-1}\text{s}^{-1} \quad \text{(R4)}$$

$$CH_3 + H \rightarrow CH_2 + H_2 k_{23} = 6.02 \times 10^{13} \exp(-15.10/RT)\text{cm}^3\text{mol}^{-1}\text{s}^{-1} \quad \text{(R23)}$$

$$CH_2 + H \rightarrow CH + H_2 k_{25} = 1.63 \times 10^{14}\text{cm}^3\text{mol}^{-1}\text{s}^{-1} \quad \text{(R25)}$$

$$CH_3 + Ar \rightarrow CH + H_2 + Ar k_{27} = 6.90 \times 10^{14} \exp(-82.50/RT)\text{cm}^3\text{mol}^{-1}\text{s}^{-1} \quad \text{(R27)}$$

$$CH_4 + H \rightarrow CH_3 + H_2 k_{28} = 1.77 \times 10^{14} \exp(-13.78/RT)\text{cm}^3\text{mol}^{-1}\text{s}^{-1} \quad \text{(R28)}$$

As the concentration of hydrogen (H_2) is significant, we have included the decomposition of H_2 as well to generate the H atoms in the reaction.

$$H_2 + Ar \rightarrow H + H + Ar k_{14} = 5.33 \times 10^{14} \exp(-96.01/RT)\text{cm}^3\text{mol}^{-1}\text{s}^{-1} \quad \text{(R14)}$$

Overall, the concentrations of all the products obtained in the simulations are found to be in good

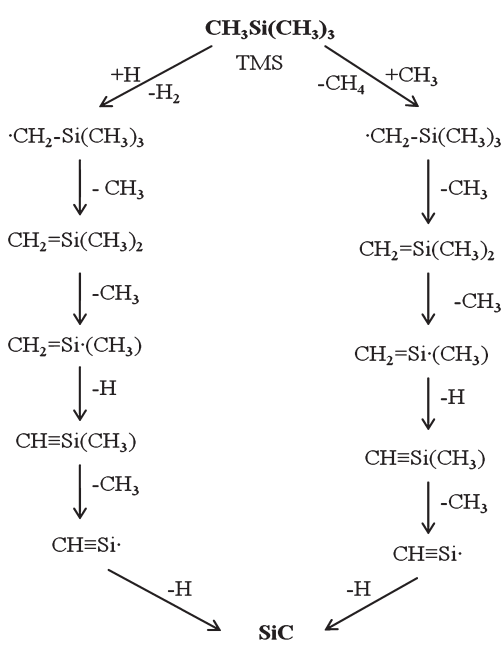

Figure 10. Suggested pathways for the formation of SiC during the thermal decomposition of TMS in single pulse shock tube experiments.

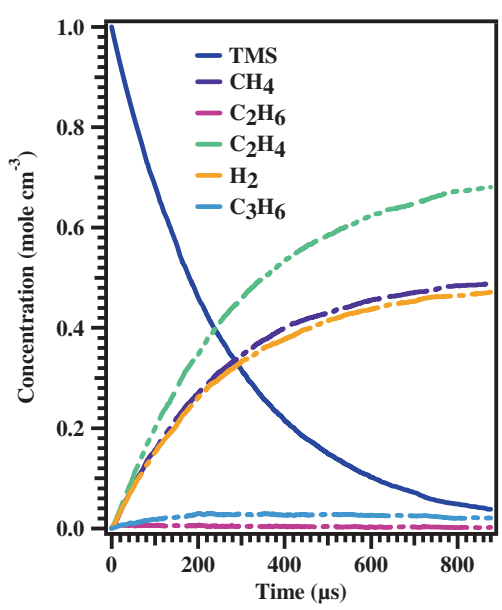

Figure 11. The distribution of concentrations of TMS and various products with respect to time when simulations were carried out using the proposed reaction scheme with the reaction time of 880 μs and the experimental temperature of 1194 K.

agreement with the experimentally measured concentrations.

Hydrogen atom and methyl radical are reactive intermediates in pyrolysis of TMS at high temperatures. These two species are responsible for the formation of SiC, probably through the following reaction mechanism. In the present work, the formation of SiC and their growth was not focused. The main aim of this study is to monitor the products formed from decomposition of TMS and their gas phase contributions to the total reaction (figure 10).

The concentration vs time profiles of reactant and the products obtained in the simulations by using the proposed reaction scheme, with the reaction time of 880μs and at experimental temperature of 1194 K is shown in figure 11. This profile shows once again the major and minor products in the thermal decomposition of TMS in the studied temperature range of 1058–1194 K.

4. Conclusions

The pyrolysis of TMS in the temperature range of 1058–1194 K was investigated, using a SPST. The main reaction products in the experiments are found to be methane and ethylene; and the minor reaction products are ethane and propylene respectively. The obtained rate coefficient for the total decomposition of TMS in the lower temperature range is k_{total} (1058–1130 K) = $(4.61 \pm 0.70) \times 10^{18} \exp(-(79.9\,\text{kcal mol}^{-1} \pm 3.5)/RT)\ \text{s}^{-1}$, and at high temperature range is, k_{total} (1130–1194 K) = $(1.33 \pm 0.19) \times 10^{6} \exp(-(15.3\,\text{kcal mol}^{-1} \pm 3.5)/RT)\ \text{s}^{-1}$. The rate coefficient obtained for the formation of methane in the studied temperature range is $k_{methane}$ (1058–1194 K) = $(4.36 \pm 1.23) \times 10^{14} \exp(-(61.9\,\text{kcal mol}^{-1} \pm 4.9)/RT)\ \text{s}^{-1}$ where R is expressed in the units of kcal K^{-1} mol^{-1}. The decomposition mechanism is proposed using 21 species and 38 elementary reactions. The concentration profiles of all the products obtained using the proposed scheme is observed to be in good agreement with the experimental findings. The C-Si bond scission is the governing reaction pathway in the complete decomposition of TMS in the temperature range of 1058–1194 K.

Acknowledgments

B.R. thanks Council of Scientific and Industrial Research (CSIR), Government of India for funding. A.P. is very grateful to CSIR for providing a research fellowship. A.P. also thank Mr. G. Sudhakar and Mr. M. Balaganesh for fruitful discussions and their help.

References

1. Herlin N, Lefebvre M, Pealat M and Perrin J 1992 *J. Phys. Chem.* **96** 7063
2. Chaussende D, Ucar M, Auvray L, Baillet F, Pons M and Madar R 2005 *Cryst. Growth Des.* **5** 1539
3. Muller S G, Brady M F, Burk A A, Hobgood H M, Jenny J R, Leonard R T, Malta D P, Powell A R, Sumakeris J J, Tsvetkov V F and Carter C H 2006 *Superattices Microstruct.* **40** 195
4. Powell J A, Matus L G, Harris G L and Yang C Y W 1989 In *Amorphous and Crystalline Silicon Carbide* Springer Proceedings in Physics Vol. 34 (Berlin: Springer)
5. Golecki I, Reidinger F and Marti J 1992 *Appl. Phys. Lett.* **60** 1703
6. Avigal Y, Schieber M and Levin R 1974 *J. Cryst. Growth* **24/25** 188
7. Chappell M J and Millman R S 1974 *J. Mater. Sci.* **9** 1933
8. Nam D H, Kim B G, Yoon J Y, Lee M H, Seo W S, Jeong S M, Yang C W and Lee W J 2014 *Cryst. Growth Des.* **14** 5569
9. Seo Y H, Nahma K S, Suh E K, Lee H J and Hwang Y G J 1997 *Vac. Sci. Technol. A* **15** 2226
10. Herlin N, Lefebvre M, Pealat M and Perrin J 1992 *J. Phys. Chem.* **96** 7063
11. Avigal Y and Schieber M 1971 *J. Cryst. Growth* **9** 127
12. Figueras R A, Garelik S, Santiso J, Rodroguez-Clemente R, Armas B, Combescure Berjoan C, Saurel J M and Caplain R 1992 *Mater. Sci. Eng. B* **11** 83
13. Seong-Min J, Kyung-Hun K, Young J Y, Myung-Hyun L and Won-Seon S 2012 *J. Cryst. Growth* **357** 48
14. Schalla R L, McDonald G E and Gerstein M 1955 *Symp. (Int.) Combust.* **5** 705
15. Gerhold B W and Inkrott K E 2006 *Combust. Flame* **146** 407
16. Cullis C F, Herron D and Hirschler M M 1985 *Combust. Flame* **59** 151
17. Wrobel A M, Czeremuszkin G, Szymanowski H and Kowalski J 1990 *Plasma Chem. Plasma Process.* **10** 277
18. Helm D F and Mack E 1937 *J. Am. Chem. Soc.* **59** 60
19. Clifford R P, Gowenlock B G, Johnson C A F and Stevenson J 1972 *J. Organomet. Chem.* **34** 53
20. Baldwin A C, Davidson I M T and Reed M D 1978 *J. Chem. Soc., Faraday Trans.* **174** 2171
21. Taylor J E and Milazzo T S 1978 *J. Phys. Chem.* **82** 847
22. Doncaster A M and Walsh R 1976 *J. Chem. Soc., Faraday Trans.* **72** 2908
23. Tschuikow-Roux E 1965 *Phys. Fluids* **8** 821
24. Tschuikow-Roux E, Sirnrnie J M and Quirring W J 1970 *Astronaut. Acta* **15** 511
25. Lifshitz A, Bauer A H and Resler E L 1963 *J. Chem. Phys.* **38** 2056
26. Rajakumar B, Reddy K P J and Arunan E 2002 *J. Phys. Chem. A* **106** 8366
27. Gaydon A G and Hurle I R 1963 In *The shock tube in high temperature chemical physics* (New York: Reinhold Publishing)
28. *Shock Waves @ Marseille I: Hypersonics, Shock Tube & Shock Tunnel Flow* R Brun and L Z Dumitrescu 1995 (Eds.) (Berlin: Springer-Verlag)
29. Bershader D and Hanson R 1987 *Astrophys. Space Sci.* **138** 426

30. Mirels H 1964 *AIAA Journal* **2** 84
31. Li S, Ren W, Davidson D F and Hanson R K 2012 In *Boundary Layer Effects behind Incident and Reflected Shock Waves in a Shock Tube* 28th International Symposium on Shock Waves (Berlin: Springer) Vol. **2** p. 471
32. Lifshitz A, Tamburu C, Suslensky A and Dubnikova F 2006 *J. Phys. Chem. A* **110** 11677
33. Manion J A and Awan I A 2013 *Proc. Combust. Inst.* **34** 537
34. Herzler J, Manion J A and Tsang W 1997 *J. Phys. Chem. A* **101** 5500
35. Rosado-Reyes C M and Tsang W 2012 *J. Phys. Chem. A* **116** 9599
36. Stranic I, Davidson D F and Hanson R K 2013 *Chem. Phys. Lett.* **584** 18
37. Skinner G B and Sokoloski E M 1960 *J. Phys. Chem.* **64** 1028
38. Hidaka Y, Higashihara T, Ninomiya N, Masaoka H, Nakamura T and Kawano H 1996 *Int. J. Chem. Kinet.* **28** 137
39. Lifshitz A, Tamburu C, Suslensky A and Dubnikova F 2004 *J. Phys. Chem. A* **108** 3430
40. Tsang W 1965 *J. Chem. Phys.* **44** 4283
41. Taylor J E, Hutchings D A and Frech K J 1969 *J. Am. Chem. Soc.* **91** 2215
42. Sivaramakrishnan R, Michael J V, Harding L B and Klippenstein S J 2012 *J. Phys. Chem. A* **116** 5981
43. Pacey P D 1973 *Can. J. Chem.* **51** 2415
44. Chemical Kinetics Simulator 1.0. 1995 IBM Almaden research center, IBM Corporation
45. Berkley R E, Safarik I, Gunning H E and Strausz O P 1973 *J. Phys. Chem.* **77** 1734
46. Oueslati I, Kerkeni B, Spielfiedel A, Tchang-Brillet W and Feautrier N 2014 *J. Phys. Chem. A* **118** 1089
47. Wang B S, Hou H, Yoder L M, Muckerman J T and Fockenberg C 2003 *J. Phys. Chem. A* **107** 11414
48. Davidson D F, Di Rosa M D, Chang E J, Hanson R K and Bowman C T 1995 *Int. J. Chem. Kinet.* **27** 1179
49. Kern R D, Singh H J and Wu C H 1988 *Int. J. Chem. Kinet.* **20** 731
50. Lifshitz A, Tamburu C and Suslensky A 1990 *J. Phys. Chem.* **94** 2966
51. Yampolskii Y P and Rybin V M 1973 *React. Kinet. Catal. Lett.* **1** 321
52. Curran H J 2006 *Int. J. Chem. Kinet.* **38** 250
53. Baulch D L, Cobos C J, Cox R A, Esser C, Frank P, Just T, Kerr J A, Pilling M J, Troe J, Walker R W and Warnatz J 1992 *J. Phys. Chem. Ref. Data* **21** 411
54. Du H and Hessler J P 1992 *J. Chem. Phys.* **96** 1077
55. Hidaka Y, Nakamura T, Tanaka H, Jinno A and Kawano H 1992 *Int. J. Chem. Kinet.* **24** 761
56. Skinner G B and Ruehrwein R A 1959 *J. Phys. Chem* **63** 1736
57. Blackmore D R and Hinshelwood C 1963 *Proc. R. Soc. London A* **271** 34
58. Knyazev V D, Bencsura A, Stoliarov S I and Slagle I R 1996 *J. Phys. Chem.* **100** 11346
59. Lim K P and Michael J V 1994 *Symp. Int. Combust. Proc.* **25** 713
60. Sivaramakrishnan R, Su M C, Michael J V, Klippenstein S J, Harding L B and Ruscic B 2011 *J. Phys. Chem. A* **115** 3366
61. Tsang W and Hampson R F 1986 *J. Phys. Chem. Ref. Data* **15** 1087
62. Markus M W, Woiki D and Roth P 1992 *Symp. Int. Combust. Proc.* **24** 581
63. Sutherland J W, Su M C and Michael J V 2001 *Int. J. Chem. Kinet.* **33** 669
64. Zhang H X and Back M H 1990 *Int. J. Chem. Kinet.* **22** 21
65. Tsang W, Cui J P and Walker J A 1990 *Proceedings of the 17th International Symposium on Shock Waves & Shock Tubes* American Institute of Physics (New York) p. 63
66. Loser U, Scherzer K and Weber K 1989 *Z. Phys. Chem.* **270** 237
67. Curran H J 2006 *Int. J. Chem. Kinet.* **38** 250
68. Konar R S, Marshall R M and Purnell J H 1968 *Trans. Faraday Soc.* **64** 405
69. Tsang W 1988 *J. Phys. Chem. Ref. Data* **17** 887
70. Zheng X B and Blowers P 2006 *Ind. Eng. Chem. Res.* **45** 530
71. Tsang W 1991 *J. Phys. Chem. Ref. Data* **20** 221